

A test bed for measuring UAV servo reliability

A. ElSaid*

Rochester Institute of Technology, Rochester, NY, 14623, USA

J. Nordlie[†] and F. El Jamiy[‡]

University of North Dakota, Grand Forks, North Dakota, 58202, USA

THE era of Unmanned aviation is flourishing and advancing in leaps and bounds jumping over all challenges and obstacles. One of the serious hinderances to the booming industry is the lack of sufficient reliability studies about the systems used on board these flying robots. Accordingly, this poses a threat to the safety and well-being of human communities as well as the loss of assets, especially in BLOS* flights. The need for a reliable endurance investigation is emerging from the fact that many of the systems and components used on UAS^{†‡} are COTS[§] which comes with scarce information, if any, about its reliability and operation-life expectancy. This topic is of vital importance to regulatory organizations to consider legalizing commercial flights that are not in the field of the human operators' line of sight. Servos are one type of these crucial components used in UAS which lack thorough reliability evaluations. This study addresses this concern through a case study of the servo used on the Boeing Insitu ScanEagle to control its ailerons. To offer the expected information about the reliability of the components, a destructive test platform was sought. A test-bed was designed to operate the servo to failure using the actual commanded positions it operates to in its real-life service. The test-bed commands the servo and logs its actual movements along with the commanded positions. These logs are used to detect the discrepancy between the commanded and actual positions to give a statistical estimate about how long the servo will endure.

I. Introduction

The UAS industry is rapidly growing and the future of aviation seems to be a natural expansion of this promising technology. One of the pillars of the success of UAS technology is the availability and cost-effectiveness of its components or sub-systems; Most UAS systems and components are within the reach of any interested organization or individual. This means that most of these subsystems are COTS that are ready to use after implementation, which makes

*Computer Science Ph.D. student and aerospace engineer, B. Thomas Golisano College of Computing and Information Sciences, aae8800@rit.edu.

[†]Computer science Instructor and UAV safety pilot, University of North Dakota, john.nordlie@und.edu.

[‡]Applied computing Ph.D. student, University of North Dakota, fatima.eljamiy@und.edu.

^{*}Beyond Line Of Sight

[†]Unmanned Aerial System(s) [drones]

[‡]Through out the paper, the term UAS is used interchangeably with UAV (Unmanned Air Vehicles)

[§]Commercial Off the Shelf

it convenient to design and construct a fully functioning UAS that meets many real-life applications. However, COTS convenience often comes with a price: they are usually sold with no-liability to limited-liability to its manufacturers. This serious problem plagues the UAS young industry and jeopardizes its path to maturity. Unlike manned air-systems, UAS's sub-systems lack the exhaustive reliability tests in general and destructive tests in particular. Thus, in most cases, there are concerns regarding the fitness of UAS to perform BLOS[¶] missions, where the aircraft is controlled, either autonomously, or remotely from no-visual-contact distance.

One of the essential components to fixed-wing UAS flight-control, to maintain a safe flight, is the device which moves its control surfaces. Electric servo motors are the most convenient choice to act as this actuating system in that it is relatively cheap, compact in size, precise, controllable, and light-weight. Though servos have all these advantages, they still dominantly suffer from limited information about reliability studies and examinations for reasons which relate to commercial competition and/or cost. Accordingly, this study is focusing on the design and implementation of a destructive testing platform to measure the life expectancy of electric servos of types which are typically used in UAS control. This work begins with a case study to pick a servo. Then a statistical analysis is performed on the servo's actual operation-angles to determine the frequency of the controlled control-surface movements. After that, the force conditions that the servo normally operates in are calculated to simulate those forces on the testing-bed. Last but not least, the test-bed and its control system were actually built for the study's experiments to command the servo angles, collect the servo's position data, and simulate the forces acting on the servo in real-time operations.

II. Related Work

Reliability study is essential in the aviation world. However, the UAV[¶] studies are still not well established. Yet, it is gaining potential because of the safety concerns raised by regulators and feasibility researchers.

Dermentzoudis [1] introduced a study about established methods to collect data to be used in evaluating UAV reliability. The study is based on data collected from military aircraft based on mass data collection from large fleets. The study focus on holistic methods rather than individual sub-systems

Uhlig *et. al.* [2] studied COTS as a cause of failure in UAV systems. The study investigated the integration of the specific sub-systems and added some redundancy to the components used to see its influence on the reliability of the UAV.

Bhamidipati *et. al.* [3] introduced an important study about COTS used in UAVs and their reliability. Though the study is intensive, the experiments were done on a single aircraft and its engine, fuel throttling, and burning system. The study can be much advanced if data were collected from several aircraft and engines of the same model to enrich the results.

[¶]Beyond Line Of Sight

[¶]Unmanned Air Vehicles

Table 1 Aircraft Specifications

Aileron Width	0.428m	Aileron Height	0.048m	Aileron Surface Area	0.021m ²
Max. Cruise Speed	50m/h	Min. Cruise Speed	40m/h	Arg. Cruise Speed	45m/h
Max. Aileron Deployment Angle (cruise)	40°				

Petritoli *et. al.* [4, 5] introduces a model that can be used to perform an overall evaluation of the reliability of the UAS systems to improve the logistics of UAV maintenance plans. The work is very well represented but still there was no mention to a reliable tool to collect the data necessary to evaluate the systems' reliability and availability.

Tan *et. al.* [6] introduced a reliability model for UAVs that considers the human factor. The study shows important results but was not much concerned with the hardware components of UAVs and how their unreliability can much affect the human operator performance.

Pan [7] investigated the use of hybrid data collection to detect anomalies which influence UAV reliability. The data collected was general performance data for the aircraft systems.

III. Case Study

The Boeing Insitu ScanEagle was picked as a case study for this work. This aircraft is a small and long-endurance UAV that can fly in BLOS operations. The aircraft aileron's electric servo motor life expectancy is the focus of this study as a case study. The aileron's positions were extracted from the aircraft's FDR**, and was used to statistically calculate the ailerons most frequent positions. This step also revealed the outliers in these positions, which are possibly errors in read signals.

A. Forces Calculation

Using the specification of the aircraft's aileron shown in Table 1, the forces exerted on the control surface by aerodynamics can be calculated. Taking the air density to be the standard sea-level density: $\rho = 1.27\text{kg/m}^3$, the forces are calculated using the equation: $F = \frac{1}{2}\rho v^2 \times \text{COS}(\theta)$ where F is the normal force on the control surface, ρ is the air density, v is the aircraft speed, and θ is the angle of the control surface to the horizontal..

B. Forces Simulation

To simulate the force acting on the control-surface, and consequently on the servo, an extension mechanical spring is used (Figure 1). The force which acts on the control-surface changes as the angle of the control-surface changes. The spring is picked so that its resistance is linear and obeys Hooks law: $F = kx$, where F : spring's resistance, k : spring's stiffness, and x : is the length of the extension of the spring. The maximum force acting on the control surface (at the

**Flight Data Recorder

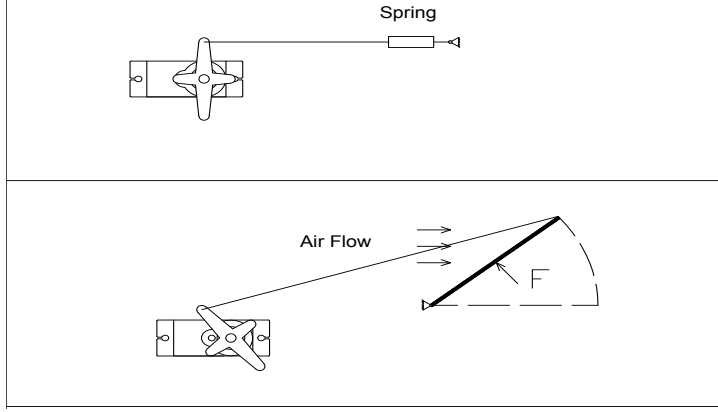


Fig. 1 Servo/Control-Surface System.

maximum deploying angle) should be covered in the maximum extension of the spring.

IV. Data Preparation

An FDR log file was used to statistically study the positions of the servo during flight. The results of this study is shown in Table 2 for the negative aileron angles, and Table 2 for the positive aileron angles. As shown, the number of positive aileron positions exceed the number of negative positions, which is expected because negative position acts as an aid for the positive position on the opposite side aileron in severe maneuvers. Figures 2a, and 2b, show the frequencies of the angles in the FDR file. The data has a 50% confidence interval $[9.84^\circ, 19.69^\circ]$ for the positive positions, and $[-11.25^\circ, -5.63^\circ]$ for the negative positions.

A list of positions is prepared to reflect the angles that the servo operate in real life and their frequencies. This list took into consideration the real-life servo operation and represented this in the number of times each position appear in the list. Table 3 depicts a sample of the prepared list based on the FDR file.

V. Implementation

The main concept with the test-bed is to let the servo operate in all the positions that are collected from the statistical study performed on the FDM file. The operations will consider the frequency of the position such the servo on the test bed will run more on the positions that occur in the real-life operations, to get a more realistic result. The servo will keep operating and its actual positions are recorded with their corresponding commanded positions, meaning the inputs and outputs of the servo will be logged. The logged data will be compared to determine the time the servo took to malfunction. As mentioned previously, the force on the servo will be simulated to achieve realistic results. The design of the platform exploits a digital rotary encoder to record the position of the servo when it reaches its commanded position.

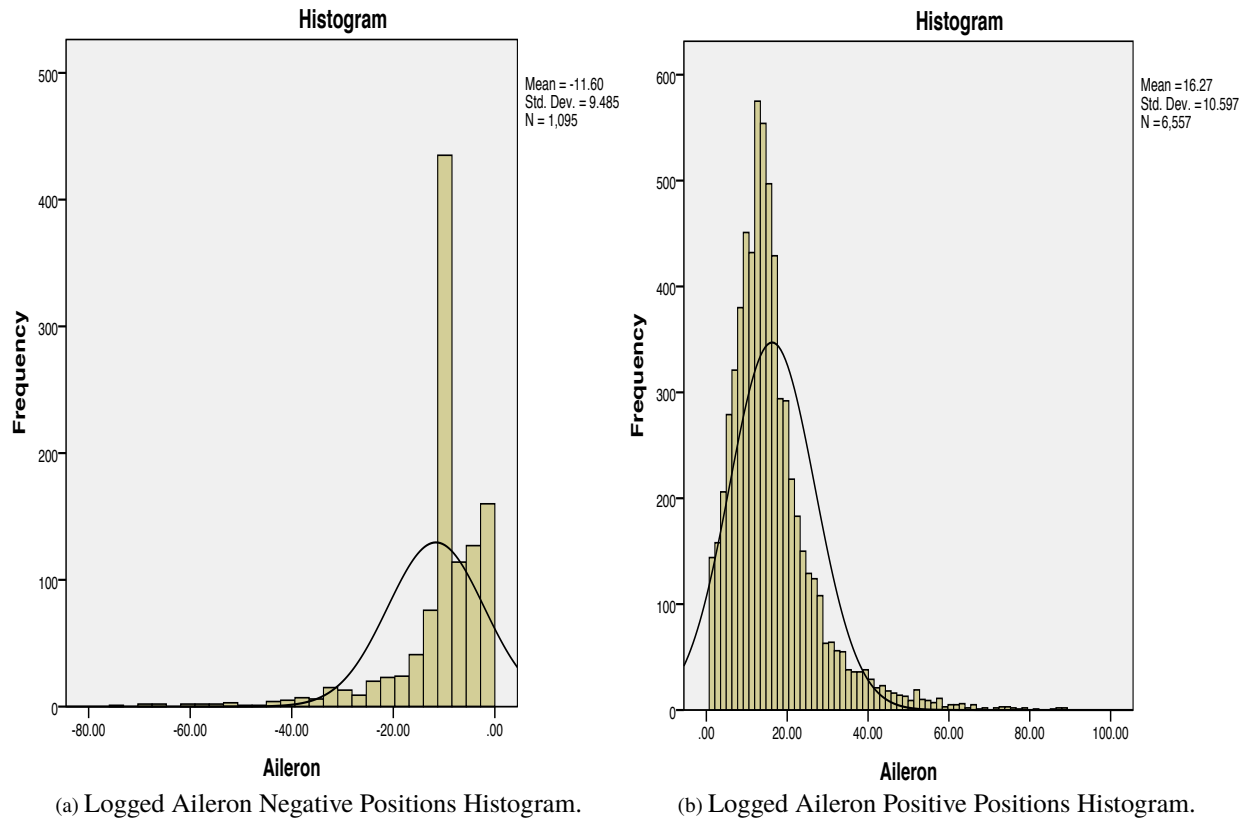


Fig. 2 Logged Aileron Positions Histograms.

Table 2 Positions Statistical Description

	Negative Positions		Positive Positions	
N	Valid	1095	Valid	6557
	Missing	0	Missing	0
Mean		-11.6022		16.2681
Std. Error of Mean		.28664		.13087
Median		-11.2503		14.0629
Std. Deviation		9.48505		10.59699
Variance		89.966		112.296
Skewness		-2.701		1.912
Std. Error of Skewness		.074		.030
Kurtosis		10.336		5.957
Std. Error of Kurtosis		.148		.060
Range		73.13		87.19
Minimum		-74.53		1.41
Maximum		-1.41		88.60
Percentiles	25	-11.2503	25	9.8441
	50	-11.2503	50	14.0629
	75	-5.6252	75	19.6881

Table 3 Commanded Positions

4	-11	13	-11	32	15	7	17	23	14	3	11
11	11	10	17	-1	-11	18	6	25	-10	25	20
11	10	7	-24	7	37	18	14	-18	-14	10	11
-4	17	35	6	3	14	28	17	34	-6	11	-30
4	13	17	21	11	15	-20	-1	24	20	6	-11
14	13	24	-25	21	8	-13	23	14	-15	3	14
17	30	31	15	-28	14	-11	15	1	27	13	-8
8	-3	-7	10	8	10	7	18	27	14	20	8
4	13	15	-17	23	-11	-3	18	8	20	13	-21
6	-27	-23	21	15	13	10	13	28	15	7	

A. Hardware

1. CAD Design

After calculating the forces acting on the servo and choosing the spring to simulate these forces, a CAD^{††} carried out to build a 3-D design for the platform. One of the major points which were considered in this step of the study was the alignment of the servo shaft and the encoder shaft. This is particularly important because any miss-alignment between the two shafts would result in additional forces, other than the ones actually acting on the servo and considered in the design.

The platform consists of a fixed base for the servo which can move on the X-Y plane. A magnet is fixed in the bottom of the base to let it move in the X-Y plane on a gallivanted steel sheet. This 2-D movement to allow adjustment to the servo position to the encoder position. The fixed base has a moving base above it where the servo is attached. The servo-base is allowed to move in the Z-direction to further adjust the servo position with respect to the encoder position. After the servo in the right position, the servo-base is tightened to restrict it from moving up and down during the test.

Figure 3a shows the CAD 3-D drawing for the platform and its internal composition. Figure 3b shows the CAD 3-D a realistic drawing for the platform. Figures 4a show the 3-D printed parts of the platform and Figure 4b shows the assembled testing-bed.

2. Microcontrollers and Computer

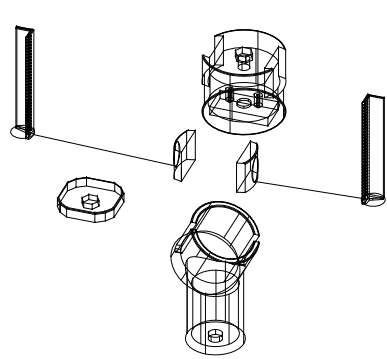
The study used two microcontrollers. The first one was used to receive input commanded servo positions (one at a time) from a computer and command the servo position by sending to the servo one position at a time. The second microcontroller was used to read the position output by the rotary encoder and send it back to the computer for logging. The two controllers have a 16 Mhz clock speed. Serial ports were used to communicate with the controllers.

3. Optical Rotary Encoder

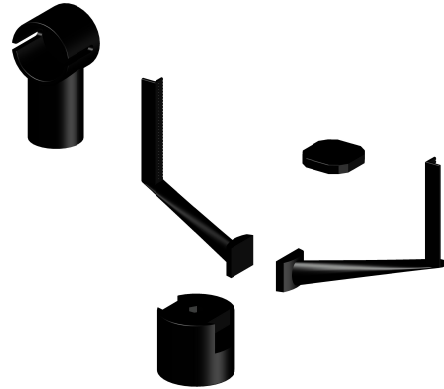
An optical rotary encoder with 1024 PPR^{##} is used to sense the actual positions of the servo as it moves to the commanded positions (Figure 5). The encoder reads the changes in angles (positions) as steps and those steps are later translated to positions (or change in positions). There are a variety of rotary encoders and the optical are more precise.

^{††}Computer Aided Design

^{##}Pulse Per Revolution



(a) 3-D Wire View.

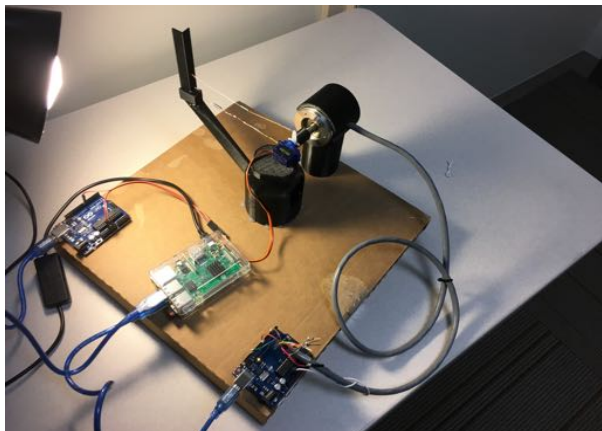


(b) 3-D Realistic View.

Fig. 3 3-D Design



(a) Disassembled Parts.



(b) Assembled Platform.

Fig. 4 3-D Printed Parts.

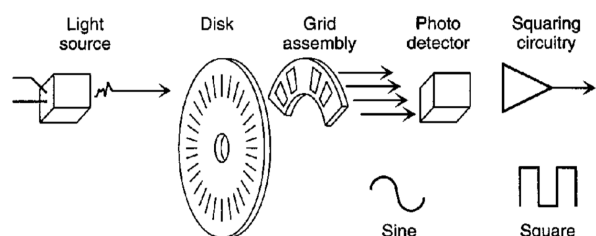


Fig. 5 Optical Rotary Encoder (adapted from [8]).

B. Embedded System

The first microcontroller is programmed to send the commanded servo positions to the servo and to maintain a uniform speed in servo motion to obtain sound readings from the rotary encoder. To keep the speed uniform, the servo positions are sent in steps of degrees to the servo in 232 milliseconds time units. When a position is successfully commanded to servo, the microcontroller sends a signal to the computer to affirm the completion of the command and the position commanded. Algorithm 1 is a snippet of the code. The program embedded in the second microcontroller reads the steps recorded by the rotary encoder and sends it to the computer. When the first microcontroller reports the completion of the command of a position, the computer records the steps counted by the encoder's microcontroller with the commanded position reported by the servo's microcontroller. Algorithm 2 is a snippet of the code.

C. Translating and Calibrating The Encoder's Signals

The rotary encoder measures the rotation using optical signals captured as the encoder's shaft rotates [8]. These measurements are dependent on the rotation speed of the shaft. In order to maintain sound readings from the encoder, the speed of the servo is maintained uniform by controlling it from the servo's microcontroller. In addition, the actual readings of the encoder are steps (pulses) and not angles. Therefore, the readings are translated to angles by referring to the first round of logging. For example, hypothetically, if the first set of commanded positions were 23, 55, 76 and its corresponding encoder reading were 98, 153, 203, then these encoder readings are fixed for these angles and later encoder readings for positions changing rounds are compared to these encoder readings. Tests are performed for several servos, and deviation from these fixed encoder readings can be easily discovered, even for the case of a factory-faulty servo.

Algorithm 1 Servo Controller

```

1: procedure SERVO_CONTROL
2:   degree  $\leftarrow$  0
3:   position  $\leftarrow$  0
4:   old_position  $\leftarrow$  0
5:   servo.move(position)
6:   i  $\leftarrow$  0
7:   position  $\leftarrow$  Get_Commanded_Position()
8:   degree  $\leftarrow$  old_positions  $-$  position
9: loop:
10:   for i  $\in$  {0, ..., absolute(degree)} do
11:     if degree  $<$  0 then
12:       servo.move(old_position + i)
13:     else
14:       servo.move(old_position - i)
15:       delay(232ms)
16:     old_position  $\leftarrow$  position
17:     Report_Complete_Command()
18:   goto loop.

```

Algorithm 2 Encoder Controller

```

1: procedure ENCODER_CONTROL
2:   counter  $\leftarrow$  0
3:   aState  $\leftarrow$  0
4:   aLastState  $\leftarrow$  digitalRead(Sensor_A)
5: loop:
6:   aState  $\leftarrow$  digitalRead(Sensor_A)
7:   if aState  $\neq$  aLastState(j) then
8:     if digitalRead(Sensor_B)  $\neq$  Sensor_A then
9:       counter  $\leftarrow$  counter + 1
10:    else
11:      counter  $\leftarrow$  counter - 1
12:      Report(counter)
13:      aState  $\leftarrow$  aLastState
14:      goto loop.
15:
16:
17:
18:

```

VI. Results

The study conducted an experiment to investigate the outcome of the designed test-bad. Although the case study considered the servo used for controlling the ScanEagle's aileron (Section III), a smaller servo was used for the

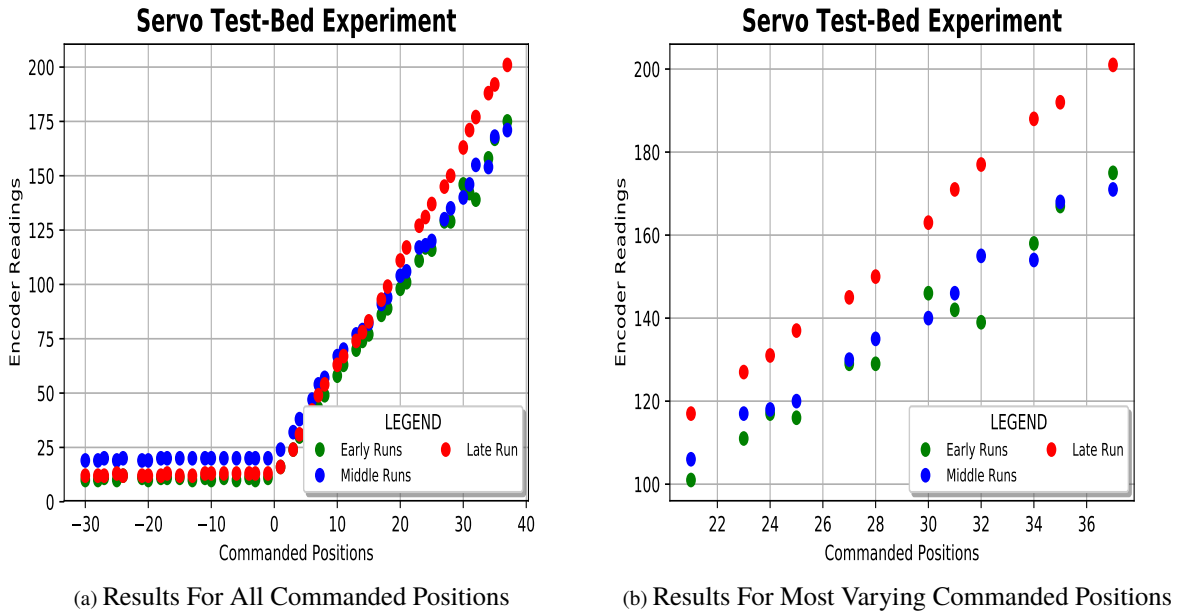


Fig. 6 Servo Test-bed Experiment

experiment just for reasons of convenience and availability. The results of the experiment are shown in Figures 6. The points in the figures represent the readings recorded for the commanded positions at the beginning (green points), the middle (blue points), and the end (red points) of the experiment. The experiment made 3649 iterations through the commanded positions set in 364 hours (≈ 15 days). To avoid the complications coming from the noise signals in the encoder's readings, the average of the first, the middle, and the last 50 iterations were used to plot the results.

In Figure 6a, the encoder readings for the negative commanded positions are showing very near to the zero value. This might be due to a fault in the servo used and/or relatively excessive spring forces (used to simulate the real-life forces), which were designed for a larger servo. Figure 6b is a zoom-in at the most varying values in the experiment phases. From the figures, the values are varying as the commanded position increases in value (larger angles), which is logical considering the increasing forces as the spring stretches (Hook's law, Section III.B). These forces simulate the real-life varying aerodynamic forces acting on the aileron, and thus the servo.

Interestingly, the results are showing that the logged angles increase as the servo operates through times rather than decreasing. Intuitively, as the servo gets older it should not be able to move to larger angles under the increasing counter forces. However, the results are showing that the deviations are positive. This might be because a servo motor, unlike a normal DC^{\$\$} motor, has an internal circuit to control its movement, which might suffer from damage as the servo ages.

^{\$\$}Direct Current

VII. Conclusion And Future Work

The test-bed considered an actual case study about a servo that is serving in one of the most successful long-endurance UAVs. The forces acting on the servo were simulated using a linearly-increasing-force extension mechanical springs. The hardware structures were CAD designed, taking into consideration the freedom of movement to align the servo shaft with the rotary encoder shaft, to alleviate any additional forces.

Later, the code used to control the system and collect the data was developed, deployed, and tested. Finally, an experiment was conducted to illustrate the outcome of the proposed system. The results showed interesting variability in the servo performance as it operates through time. Though the servo did not completely fail, a slight difference in the commanded position can result in a devastating situation as a UAV maneuvers.

For future work, some hardware can be enhanced. The apparatus used copper wires to attach the servo to the springs, which is not ideal as copper might be more malleable than desired. Therefore, a stiffer material can be used. Also, the fixation of the servo base can be better designed.

Further, additional experiments shall be carried out on a collection of servos of the type used on the UAV subject of the introduced case-study. This shall be used for a statistical study to enhance and support the findings, which might offer useful information for the operators of one of the most successful UAVs in unmanned aviation.

References

- [1] Dermentzoudis, M., "Establishment of models and data tracking for small UAV reliability," Tech. rep., NAVAL POSTGRADUATE SCHOOL MONTEREY CA, 2004.
- [2] Uhlig, D., Bhamidipati, K., and Neogi, N., "Safety and reliability within UAV construction," *25th Digital Avionics Systems Conference, 2006 IEEE/AIAA*, IEEE, 2006, pp. 1–9.
- [3] Neogi, N., Bhamidipati, K., Uhlig, D., Ortiz, A., and Krauss, J., "Engineering safety and reliability into UAV systems: mitigating the ground impact hazard," *AIAA Guidance, Navigation and Control Conference and Exhibit*, 2007, p. 6510.
- [4] Petritoli, E., Leccese, F., and Ciani, L., "Reliability and Maintenance Analysis of Unmanned Aerial Vehicles," *Sensors*, Vol. 18, 2018, p. 3171. doi:10.3390/s18093171.
- [5] Petritoli, E., Leccese, F., and Ciani, L., "Reliability degradation, preventive and corrective maintenance of UAV systems," *2018 5th IEEE International Workshop on Metrology for AeroSpace (MetroAeroSpace)*, IEEE, 2018, pp. 430–434.
- [6] Tan, Y., Feng, D., and Shen, H., "Research for Unmanned Aerial Vehicle components reliability evaluation model considering the influences of human factors," *MATEC Web of Conferences*, Vol. 139, EDP Sciences, 2017, p. 00221.
- [7] Pan, D., "Hybrid data-driven anomaly detection method to improve UAV operating reliability," *Prognostics and System Health Management Conference (PHM-Harbin)*, 2017, IEEE, 2017, pp. 1–4.
- [8] Considine, D. M., "Process instruments and controls handbook," *McGraw-Hill*, 1957.